Two Port Calibration Insensitive to Flange Misalignment

Alexander Arsenovic, Robert M. Weikle II, Jeffrey Hesler

***Abstract*—As waveguide measurements continue to push upwards in frequency, waveguide misalignment becomes a severe problem. In this paper we present an alternative, slightly more general formulation of a reflectometer calibration resistant to flange misalignment. This new solution is used in combination with the well known Unknown Thru algorithm to create a two-port calibration insensitive to flange misalignment. The resultant calibration algorithm, termed MRC, is tested both numerically and experimentally. While the numerical simulation show that MRC works as intended, the experimental results indicate that there are other measurement errors which need to be taken into account.**

I. Introduction

AS waveguide measurements continue to push upwards in frequency, waveguide misalignment caused by mechanical tolerances becomes a severe problem[1]. Not only does misalignment produce reflections at each flange connection, but it creates measurement inaccuracies by inducing calibration error[2], [3]. While improving the mechanical alignment mechanism is being addressed by the IEEE P1875 working group[4], new calibration algorithms have been developed to operate in the presence of such misalignment[5]. The original solution to a reflectometer calibration utilizing delayed shorts of unknown phase was given in [6]. Lui and Weikle helped to generalize this solution by allowing the load to be arbitrary[5]. Their formulation, coupled with the modeling of a radiating rectangular waveguide [7], produced a one-port calibration that was insensitive to flange misalignment. This algorithm has been referred to by the acronym SDDL, an acronym for the standard set; Short Delay Delay Load.

While one-port measurements are of interest, full two-port capabilities are desirable. Currently, two-port calibrations at frequencies above 100GHz, are generally made using either SOLT, or TRL. Above 500GHz, the quarter-wave line required by TRL becomes difficult to manufacture and use without damage. The accuracy of measurements corrected using these algorithms depends on the ability to realize either perfectly matched transmission standards, or precisely known reflect standards. By combining the SDDL technique[5] with the Unknown Thru [8], a two-port calibration insensitive to flange misalignment is possible. As a byproduct, this algorithm yields a direct measurement of the flange alignment. It is acknowledged that a calibration insensitive to flange misalignment will not correct for the misalignment present in subsequent measurements. It will however eliminate flange misalignment as source of calibration error, an important step towards improving measurement accuracy in the waveguide medium.

This paper is organized as follows. In Section II we present a simplified and slightly more general derivation for the SDDL one-port calibration which doesn't require a flush short. This subtle improvement allows SDDL to be applied in mediums where flush shorts are not available. Furthermore, the new derivation yields the unknown delay phases directly without determining the calibration error parameters, allowing SDDL to be easily added into existing calibration software. In Section III a procedure to combine SDDL with the industry standard Unknown Thru algorithm is described, thereby producing a two-port calibration insensitive to flange misalignment. The resultant algorithm, termed Misalignment Resistant Calibration (MRC somethign else?), is verified numerically as well as tested experimentally in rectangular waveguide at 325-500GHz (WR-2.2, WM-??). Section V evaluates MRC by way of comparison against the industry standard 12-term and Unknown Thru calibrations. This comparison is made through a set of verification standards.

II. Reflectometer Calibration with unknown lossless reflects

From a mathematical perspective, the problem of one-port calibration is the determination of a Mobius transformation by observing how a known set of points is altered

by the transformation. It is well known that three points uniquely determine the parameters of the transform[9]. If more than three points are observed, it is possible to exchange the exact location of every point with different constraints. The SDDL solution employs two lossless delay shorts of unknown phase. When s-parameters are used, this physical constraint implies that the short, and two delay shorts all lie on a common circle. Enforcing this constraint algebraically leads to an involved solution[5]. An simplified solution is possible by analyzing the problem in the impedance domain.

A. General Solution

The problem of calibration is generally solved in the language of scattering or transfer parameters but can equally well be solved in alternative domains such as impedance or admittance[10]. The fact that the actual measurement hardware is based upon scattering parameters is irrelevant. Translating to and from different network representations amounts to a change of basis. For this formulation of SDDL we choose to work with impedance parameters because it makes the lossless constraint simple to enforce, ie $\Re\{z\} = 0$. In effect, this transforms the constraint that points lay on a circle with the constraint that points are collinear.

The measured input impedance of a load embedded behind a two-port network is given by[11].

$$\mathbf{z_{in}} = z_{11} - \frac{z_{12}z_{21}}{z_{22} + \mathbf{z_l}} \tag{1}$$

Where z_{ij} are the impedance parameters of the embedding network, and $\mathbf{z_l}$ and $\mathbf{z_{in}}$ are the load and input impedance, respectively. This can be put into the standard form of a Mobius transformation by treating the determinant of the impedance matrix as a single variable,

$$\mathbf{z_{in}} = \frac{\mathbf{z_l} + \Delta z}{\mathbf{z_l} + z_{22}} \tag{2}$$

where Δz is the determinant of the two-port impedance matrix. For our purposes, this formula is only used to demonstrate that the functional relationship between input and load impedance is a Mobius transformation.

To determine the phases of the two lossless delay-shorts, we make use of the fact that a mobius transformation leaves the cross-ratio invariant [9]. It is noted in passing that the usefulness of this property has be emphasized in the past [12]. The cross-ratio between four complex numbers is defined by,

$$[a, b, c, d] \equiv \frac{(a-b)(c-d)}{(a-d)(c-b)} \tag{3}$$

A mobius transformation leaves this quantity unchanged, which implies that the cross-ratio between any four input and load impedances are equal. Representing all input impedance values with an apostrophe this invariance is expressed by,

$$\frac{(a'-b')(c'-d')}{(a'-d')(c'-b')} = \frac{(a-b)(c-d)}{(a-d)(c-b)} \tag{4}$$

Since all the input impedances are observable through measurement, their cross ratio may all be lumped into a single complex number z, which is known.

$$z = \frac{(a-b)(c-d)}{(a-d)(c-b)} \tag{5}$$

Let a and b represent the impedances of the two delay shorts, and c and d represent the impedances for the two fully known standards. The goal is to solve for a or b in terms of the other variables. Cross multiplying (5) and grouping terms alike in a and b.

$$a\underbrace{(c-d-cz)}_{e} + b\underbrace{(d-c-dz)}_{f} + abz + \underbrace{cdz}_{g} = 0 \tag{6}$$

Making the substitutions $e = (c-d-cz)$ and $f = (d-c-dz)$, all of which are known, we have.

$$ae + bf + abz + g = 0 \tag{7}$$

Solving for a, illustrates that a and b are related by a mobius transformation.

$$a = -\frac{fb+g}{zb+e} \tag{8}$$

Assuming a and b are delay shorts, their impedances will be purely imaginary. Therefore, a and b are each one-dimensional, and (8) may be interpreted geometrically as describing the intersection of a line and a circle[13], as illustrated in Figure 1. The constraints that a and b are purely imaginary may be enforced algebraically by applying $-a = \bar{a}$ and $-b = \bar{b}$ to (8).

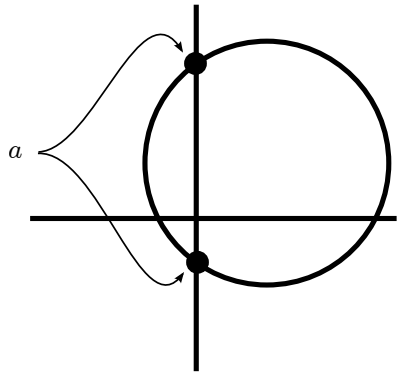

Figure 1. Geometry of problem

$$\begin{aligned} -a &= \bar{a} \\ \frac{fb+g}{zb+e} &= \frac{\bar{f}b-\bar{g}}{-\bar{z}b+\bar{e}} \\ (fb+g)(-\bar{z}b+\bar{e}) &= \left(\bar{f}b+\bar{g}\right)(zb+e) \end{aligned} \tag{9}$$

expanding yields a quadratic in b

$$\begin{aligned} b^2\left(-f\bar{z}-\bar{f}z\right)+b\left(-g\bar{z}+\bar{g}z+f\bar{e}-\bar{f}e\right)+ & \\ +\left(g\bar{e}+\bar{g}e\right) &= 0 \end{aligned} \tag{10}$$

$$b^2\underbrace{\Re\left(-f\bar{z}\right)}_{A}+b\underbrace{j\Im\left(\bar{g}z+f\bar{e}\right)}_{B}+\underbrace{\Re\left(g\bar{e}\right)}_{C} = 0 \tag{11}$$

Replacing the polynomial coefficients with A, B, and C allows (11) to be solved for b

$$b=\frac{-B\pm\sqrt{B^2-4AC}}{2A} \tag{12}$$

Once b is found then a may be found directly from (8). An approximate value of b and/or a, is required to determine the correct sign in the radical.

Evaluating (12) from measured s-parameter data, requires the data first be transformed into the impedance domain. This can be done with the familiar formula.

$$z=\frac{s+1}{-s+1} \tag{13}$$

Once both a and b are determined, they may be transformed back into reflection coefficient values by the inverse transform,

$$s=\frac{z-1}{z+1} \tag{14}$$

It is interesting to note that the cross-ratio invariance allows for the determination of the partially defined calibration standards without having to solve for the transformation parameters, ie the error parameters of the calibration. Once the partially known calibration standards are determined, a tradition one-port calibration algorithm which accepts four standards can be employed. This makes SDDL easy to add as an additional feature to existing calibration software.

B. Special Case of flush short (SDDL)

It is instructive to compare the new formulation with previously derived specific cases to gain some perspective. The most recent solution, given in [5], assumes the availability of a flush short. This implies that either c or d will be 0, which by (6) yields $g=0$. Reflecting on this condition geometrically, (8) becomes,

$$a=\frac{-fb}{zb+e} \tag{15}$$

When $b=0$, $a=0$ and thus, the right hand side represents a circle that passes through the origin and the imaginary axis, as shown in Figure 2. Given that $a\neq 0$, or else the cross ratio would collapse, a must be the other point of intersection. This is a unique solution, so no sign choice must be made to evaluate b.

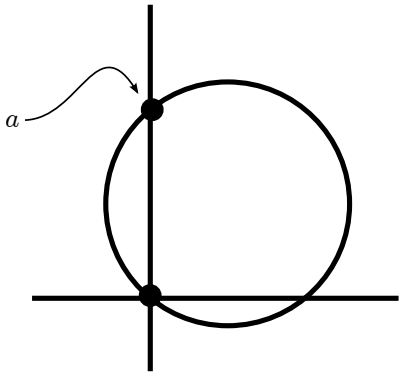

Figure 2. Geometry of problem when a flush short is used.

Working through the algebra, (11) simplifies to,

$$b^2\Re\left(-f\bar{z}\right)+bj\Im\left(f\bar{e}\right) = 0$$

The solution for b is then,

$$b=j\frac{\Im\left(f\bar{e}\right)}{\Re\left(f\bar{z}\right)} \tag{16}$$

Again, once b is found then a may be found directly from (8). While this solution is valid, an more concise solution without intermediary variables is possible. Starting with the cross ratio

$$z = \frac{(a-b)(c-d)}{(a-d)(c-b)} \tag{17}$$

Chose d to represent the short, so that $d = 0$, and rearrange the cross ratio as such,

$$\begin{aligned} z &= \frac{(a-b)c}{a(c-b)} && (18)\\ z - zbc^{-1} &= \frac{a-b}{a} && (19) \end{aligned}$$

Now, since a and b are purely imaginary, the right hand side of this is purely real,

$$\begin{aligned} \Im(z - zbc^{-1}) &= 0 && (20)\\ \Im(z) &= \Im(zbc^{-1}) && (21) \end{aligned}$$

The b may be factored out by using it's anti-symmetry with respect to conjugation,

$$\begin{aligned} \Im(z) &= \frac{1}{2j}\left(bzc^{-1} - \overline{b}\overline{z}\overline{c}^{-1}\right) && (22)\\ \Im(z) &= \frac{1}{2j}b\left(zc^{-1} + \overline{z}\overline{c}^{-1}\right) && (23)\\ b &= j\frac{\Im(z)}{\Re\left(zc^{-1}\right)} && (24) \end{aligned}$$

One can determine a by (8), or through a similar expression by calculating a different cross ratio with the variables a and b swapped. Such as ,

$$a = j\frac{\Im(z_a)}{\Re\left(z_a c^{-1}\right)}, \qquad z_a = \frac{(b-a)(c-d)}{(b-d)(c-a)} \tag{25}$$

C. Special Case of flush short and perfect match(SDDM)

Next, to examine the original solution[6] which assumed a flush short and a perfect matched load. Given this set of standards the general method of solving the roots of the quadratic in (11) may be unstable due to the match standard having infinite impedance. We have found that the accuracy of the solution depends on the numerical approximation to infinity, which is undersireable. A simple workaround can be made as follows. Starting with the cross ratio

$$z = \frac{(a-b)(c-d)}{(a-d)(c-b)} \tag{26}$$

Chose d to represent the short and c to represent the match, so that $d = 0$ and $c = \infty$. The trick for a stable solution is to isolate c in a denominator,

$$\begin{aligned} z &= \frac{(a-b)c}{a(c-b)} && (27)\\ zac - zab &= ac - bc && (28) \end{aligned}$$

Dividing by the c, and taking the limit as $c \to \infty$

$$\begin{aligned} za - \frac{zab}{c} &= a - b && (29)\\ b &= a(1-z) && (30) \end{aligned}$$

This equation is dope.

D. Conclusion and Extension

Through the usage of the cross ratio, an approach to one-port self calibration has been given. The method requires two fully known standards, and two partially determined standards which have known values in one dimension. By changing circuit representations, or any conformal transformation for that matter, this constraint may be adjusted until it is convenient to enforce. It has been shown that previously derived solutions are specific cases in which the known standards had values of 0 and/or ∞ in the impedance domain.

The applications of one-port self-calibration may be characterized by the number of fully known standards employed. Given that there are 6 degrees of freedom in a conformal transformation acting on 2-dimensional space, the following schemes are possible,

- >3 knowns (Overdetermined Least Squares)
- 3 knowns (Standard SOL)
- 2 knowns + 2 half knowns (This paper)
- 1 known + 4 half knowns (To-be-done)

There may be better ways to categorize one-port calibrations, but this scheme seems a reasonable first draft. It is also noted, though not explored, that the method presented here could most certainty be simplified and extended through the use of geometric conformal algebra[14].

III. Two-port Calibration (UnknownThru)

While SDDL can tolerate misalignment on reflect standards, at least one transmissive connection is needed to correct two-port measurements. The calibration algorithm known as *Unknown Thru*[8] provides precisely the self-calibration capabilities needed to handle misalignment on the thru standard. Specifically, the Unknown Thru requires that the *thru* standard be reciprocal and have

a transmission phase known within π. The exact s-parameters of the standard are not required. The Unknown Thru algorithm can be broken up into three discrete steps:

1) One-port calibration on port 1 (yields 3 -terms)
2) One-port calibration on port 2 (yields 3 -terms)
3) Measurement of reciprocal Thru (yields 1-term)

The Misalignment Resistant Calibration (MRC) is created by modifying the UnknownThru to use the SDDL solution described in the previous section for steps 1 and 2. The third step is described in [8], and need not be repeated here.

A. Implementation and Availability

The SDDL, MRC, and other conventional algorithms have all been implemented as part of the open-source python module scikit-rf[15]. All algorithms have been tested numerically with a linear circuit simulation to verify the solutions are correct and stable. Details of the numerical verification is described in the following section.

IV. Simulation

A. Numerical Verification

The Unknown Thru is part of a family of calibration algorithms known as the error box model, or 8-term model [16], [17]. In this model, the true response of a two-port device $\mathbf{T}$ is embedded within unknown networks $\mathbf{X}$ and $\mathbf{Y}$, illustrated in Figure 3. As is common to most applications employing the error-box model, the s-parameters are transformed into wave cascading matrices which allows the combined response to be calculated through matrix multiplication.

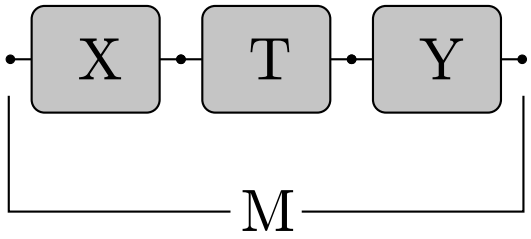

Figure 3. Diagram of the error box model

The relation between the true response of a two-port and it's measured response is expressed algebraically by

$$\mathbf{M} = \mathbf{XTY} \tag{31}$$

Where

- $\mathbf{M}$ is the measured response
- $\mathbf{T}$ is the true response
- $\mathbf{X}, \mathbf{Y}$ is the embedding networks representing the intervening circuitry

In simulation, all of the networks $\mathbf{M}, \mathbf{T}, \mathbf{X}$ and $\mathbf{Y}$ are observable, which allows the accuracy of the calibration algorithm to be verified.

A calibration is tested as follows. First, random matrices are created for the error networks $\mathbf{X}$ and $\mathbf{Y}$. Next, the appropriate set of calibration standards $\{\mathbf{T}\}$ are sandwiched in between the $\mathbf{X}$ and $\mathbf{Y}$, producing a corresponding set of fictitious measurements $\{\mathbf{M}\}$. The algorithm under test is given the measurement set $\{\mathbf{M}\}$, and the assumed ideal responses $\{\mathbf{I}\}$. For self-calibration algorithms, such as the UnknownThru, SDDL, and MRC, the ideal standards are different from their true response, ie $\{\mathbf{T}\} \neq \{\mathbf{I}\}$. For example, to correctly test SDDL, it was given an ideal standard set containing delay shorts of lengths 45° and 90°, while the actual responses used to generate the corresponding measurements where of lengths 30° and 120°.

Once a calibration algorithm has run, it can produce a corrected response from a measured device under test (DUT). For an algorithm to be considering working, it must correctly determine, inasmuch as possible, the parameters of the embedding networks $\mathbf{X}$ and $\mathbf{Y}$ as well as random DUTs within a reasonable numerical accuracy. This entire process is built into the calibration test-suit of scikit-rf.

While numerical simulation may be used to verify that an algorithm is producing a valid solution, it also provides a way to model experimental measurements. In the next section, an experimental comparison of the SOLT, UnknownThru and MRC is given, followed by a simulation of expected results.

V. Experiment and Simulation

A. Measurement Procedure

To test the calibration algorithm measurements were made in the 325-500GHz (WR-2.2 , WM-?) frequency band using a pair of Virginia Diodes extender heads (VNAX TXRX-TXRX), driven by a Agilent PNA-X. The flanges at the test ports were altered by reaming out the alignment holes to a diameter of .0066" to induce a larger amount of misalignment. The resultant amount of alignment tolerance was chosen to equal the flange's designed tolerances when used in the WR-1.0 (WM-250)

band, i.e. the worst-case expected misalignment. In order to prevent the need to ream out the calibration standards, the alignment pins were removed from the test-port flanges. A picture of the modified test-ports is shown in Figure 4 .

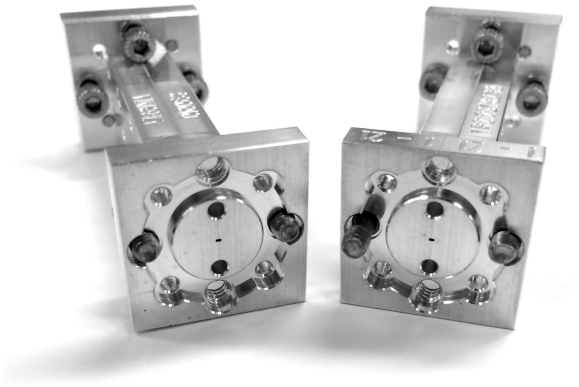

Figure 4. Picture of the test-ports with alignment pins removed.

The MRC calibration was created from measurements a flush short, two delay shorts (realized with delay shims), the radiating open, and a flush thru. Because pins were removed from the test-ports, as described in Section V-A, the inner dowel holes were used to provide alignment during the thru measurement. For comparison, 12-term and Unknown Thru algorithms were created from the identical measurement data with the exception that the radiating open was replaced by a matched load. In order for the calibration kits to be as similar as possible, four reflect standards were used in both the 12-term and Unknown Thru calibrations. Both of these calibrations used an overdetermined least squares algorithm similar to that described in [18] for the one-port stages of calibration.

Although various metrics have been used to demonstrate calibration quality, we find the measurement of verification standards to be the most interpretable and relevant. A series of devices were measured and corrected using all three of the calibrations, producing a set of data which can be directly compared. Both transmissive and reflective devices were measured to accurately represent the algorithms performance on a whole. These results are shown in Figures 6-8.

B. Results

Figure 6 shows the corrected reflection coefficient from a 1" straight waveguide terminated with a flush short on the far port. Also shown is the theoretical response of an ideal rectangular waveguide 1" long with finite conductivity on the waveguide walls. A resistivity of $2.8e^{-8}\Omega m$, and surface roughness of $.05\mu m$ RMS was chosen as reasonable values which most closely match the measurements. Both 12-term and Unknown Thru produce identical responses, as is expected for non-transmissive devices. All traces are similar with the exception that MRC produces a smaller ripple at the lower end of the band.

Figures 7 and 8 show the corrected response of a 1" straight waveguide measured in transmission. Figure 8 demonstrates that MRC shows the best agreement with the theoretical response. It can be seen that the 12-term algorithm produces high frequency ripples of about $\pm.5$dB, about the theoretical response, while the Unknown through algorithm has a different frequency dependence and minor ripple.

C. Modeling results through simulation

Figures 9 through 11 are simulations corresponding to the measurements in Figures 6-8. A numerical simulation, as described in Section IV was constructed, and the true calibration standards where perturbed heuristically until simulated results agreed with the measurements. In these simulations the embedding networks $\mathbf{X}$ and $\mathbf{Y}$ were taken from a previous calibration, created from with experimental measurements. The exact responses of $\mathbf{X}$ and $\mathbf{Y}$ are not needed to capture the general effects, just their approximate values.

The *true* calibration standards were perturbed by cascading a model of the misaligned flange in front of the delay shorts, and thru standard. An equivalent circuit for the misaligned flange can be coarsely approximated by shunt susceptance[19], as shown in figure 5. More sophisticated models of waveguide misalignment produce frequency-dependent values for the susceptance, but for our purposes, simple lumped circuit elements are sufficient. The nominal values of the shunt capacitance and inductance can be chosen based upon the expected amount of misalignment. These values were then adjusted within reason until agreement with measurements was achieved. Eventually, values of 2fF and 4nH where were chosen.

In addition to the flange perturbations, zero-mean white gaussian phase noise was added to the fictitious measurements. To accurately reflect observed noise characteristics, different amounts of noise was added to the transmission than to the reflective s-parameters. In summary, values

chosen for the adjustable parameters used in the simulation were,

- $\sigma_{\angle S_{ij}} = .8°$
- $\sigma_{\angle S_{ii}} = .2°$
- C = 2fF
- L = 4nH

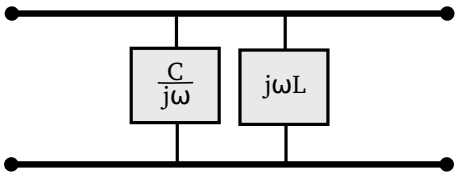

Figure 5. Circuit model used to approximate a misalignment flange .

D. Observations

By comparing figures 6-8 with figures 9-11 it is clear that the simulated performance of the MRC algorithm is substantially better than the measured results. This suggests the existence of additional sources of uncertainty other than flange misalignment. Some specific comments about the results:

- It was not possible to degrade MRC's corrected results given the types of perturbations used in this simulation. One exception is the reflection from an ideal 1" waveguide, as shown in figure 10. MRC's result is directly proportional to the amount of phase noise in the simulation.
- MRC's corrected response in figure 6 differs greatly from the simulation in figure 9.
- Regarding the theoretical responses in figures 6 and 13: It was not possible to simultaneous achieve the best fit between theory and measurement, given a single value for waveguide loss and roughness. The cause of this discrepancy is unknown.

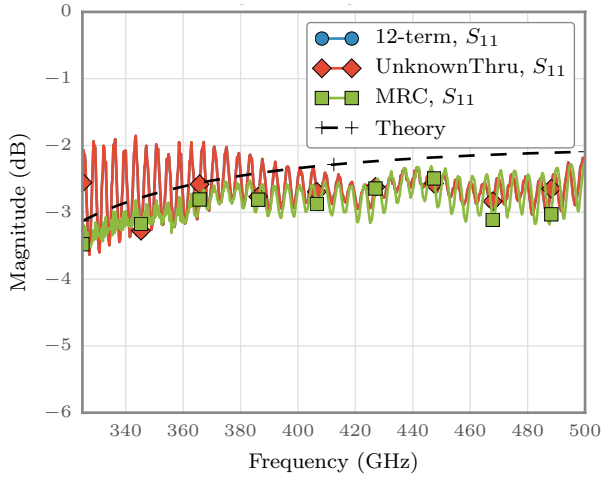

Figure 6. Corrected measurement of the reflection coefficient from a 1" straight waveguide terminated with a short (SOLT and UnknownThru, produce identical results as expected)

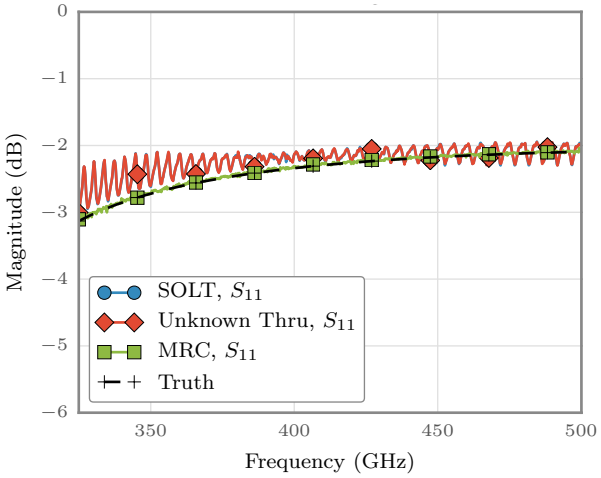

Figure 9. Simulation of corrected measurement of the reflection coefficient from a 1" straight waveguide terminated with a short (SOLT and UnknownThru, produce identical results as expected)

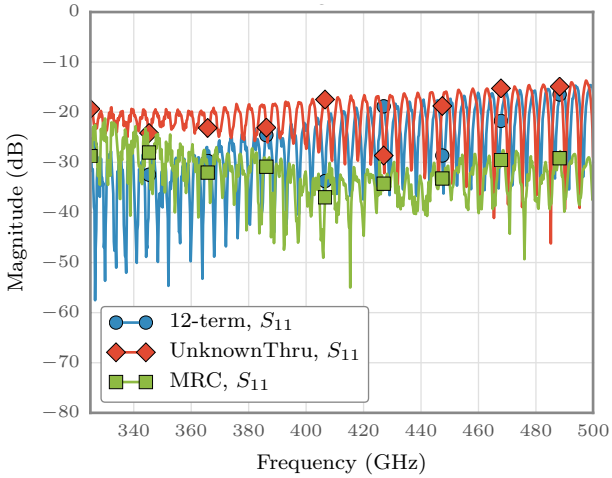

Figure 7. Corrected measurement of the reflection coefficient from a 1" straight waveguide

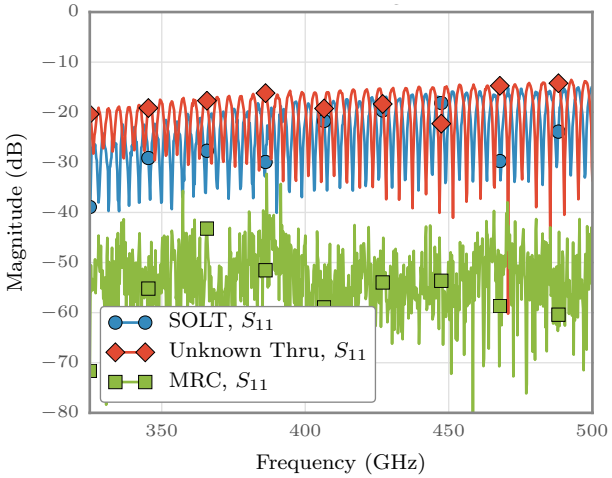

Figure 10. Simulation of corrected measurement of the reflection coefficient from a 1" straight waveguide

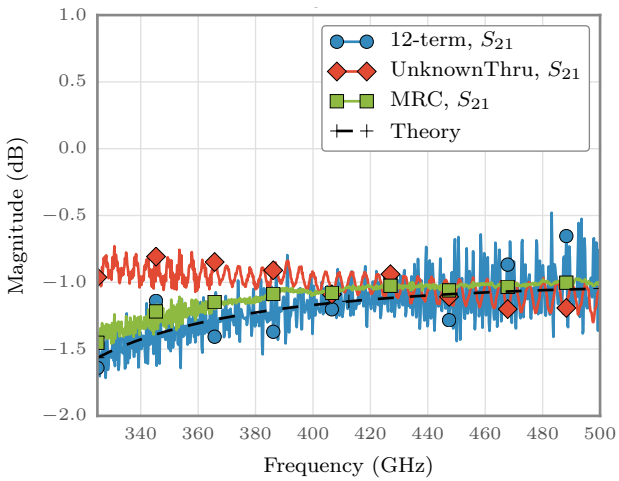

Figure 8. Corrected measurement of the transmission coefficient through a 1" straight waveguide

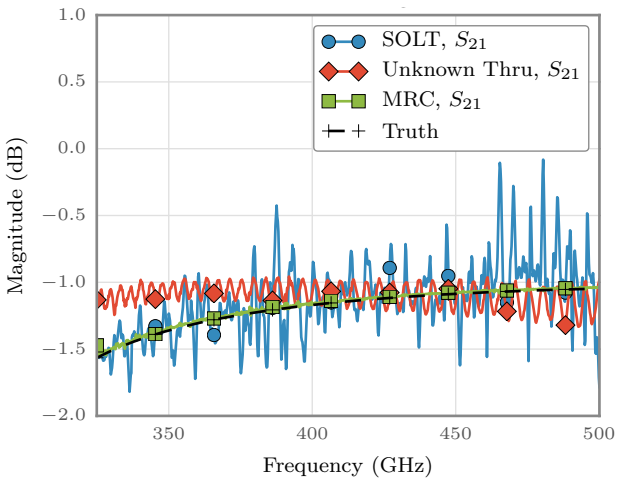

Figure 11. Simulation of corrected measurement of the transmission coefficient through a 1" straight waveguide

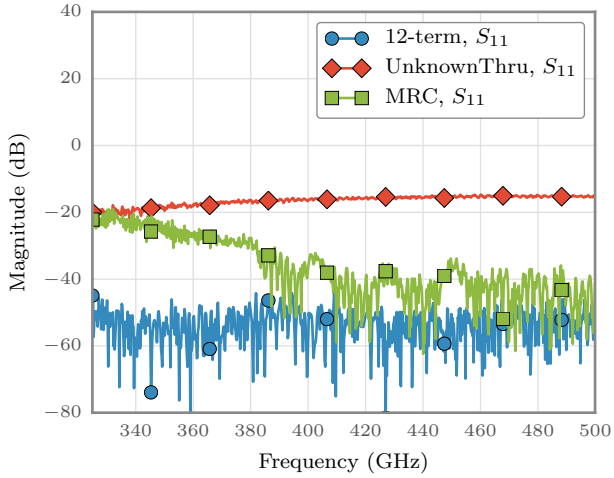

Figure 12. Corrected measurement of the reflection coefficient from a flush thru connection

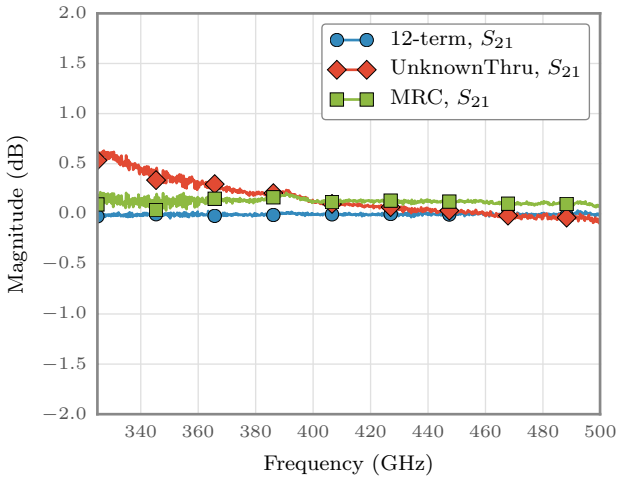

Figure 13. Corrected measurement of the reflection coefficient from a flush thru connection

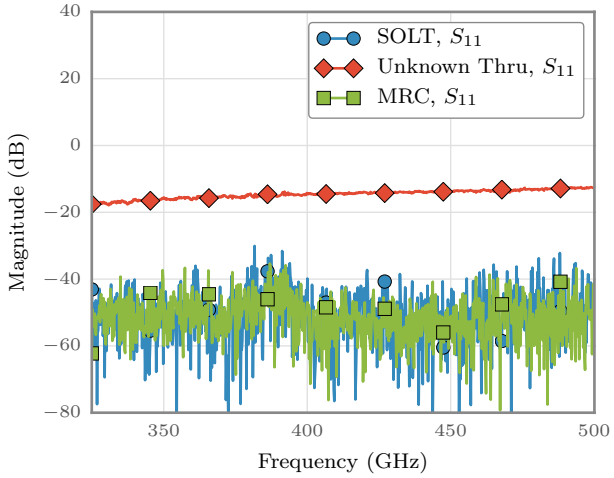

Figure 14. Simulated measurement of the reflection coefficient from a flush thru connection

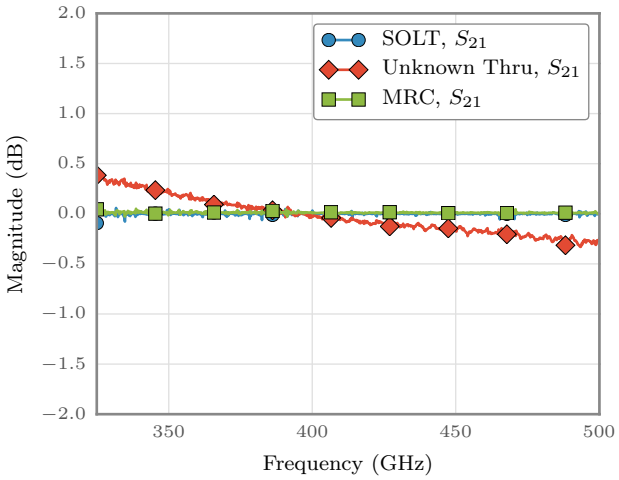

Figure 15. Simulated measurement of the reflection coefficient from a flush thru connection

E. Absolute measurement of the flange misalignment

A unique characteristic of MRC algorithm is it's ability to measure the absolute flange misalignment between a pair of test-ports. In an attempt to demonstrate this, the flush through was measured a second time, without being used in the calibrations. The reflection and transmission coefficient of the flush through is shown in figures 12 and 13, respectively. Note that the result of the 12-term calibration is expected to be very close to ideal, as it is only a measure of repeatability. The 12-term response does yield a way to estimate an appropriate noise level. Accompanying simulations of a perfect flush thru are shown in figures 14 and 15.

F. Summary

Although the MRC calibration appears to improve calibration quality for some verification standards, these improvements are less than expected from corresponding simulations. The inconsistency between simulated and measured performance indicate that there are other problems with the measurement system beyond flange misalignment.

VI. Conclusion

We have presented an alternative, slightly more general formulation of the SDDL algorithm utilizing the cross-ratio. This solution is used in combination with the Unknown Thru to create a two-port calibration insensitive to flange misalignment. The resultant calibration algorithm, termed MRC, has been testing both numerically and experimentally. While the numerical simulation show that MRC works as intended, the experimental results indicate that there are other measurement errors which need to be taken into account.

Although the MRC, and SDDL algorithms are designed to operate in the presence of flange misalignment, they may be applicable to other measurement mediums and scenarios where similar partially known reflective standards are advantageous. All algorithms have been implemented and tested as part of the open-source python module scikit-rf.

References

[1] E. W. A. R. Kerr and N. Horner, "Waveguide flanges for alma instrumentation," Nov 1999.

[2] A. Arsenovic and R. Weikle, "Comparison of competing designs for delay-short calibration standards at wr-1.5," *International Conference on Infrared, Millimeter, and Terahertz Waves*, September 2012.

[3] D. F. Williams, "500 GHz - 750 GHz rectangular-waveguide vector-network-analyzer calibrations," *Terahertz Science and Technology, IEEE Transactions on*, vol. 1, pp. 364 –377, Nov. 2011.

[4] N. Ridler, "IEEE begins work on waveguide standards above 110 GHz [MTT-S society news]," *IEEE Microwave Magazine*, vol. 10, p. 122, Feb. 2009.

[5] Z. Liu and R. Weikle, "A reflectometer calibration method resistant to waveguide flange misalignment," *Microwave Theory and Techniques, IEEE Transactions on*, vol. 54, pp. 2447 –2452, June 2006.

[6] W. Sigg and J. Simon, "Reflectometer calibration using load, short and offset shorts with unknown phase," *Electronics Letters*, vol. 27, pp. 1650 –1651, aug. 1991.

[7] D. F. Williams, M. T. Ghasr, B. Alpert, Z. Shen, A. Arsenovic, R. M. Weikle, and R. Zoughi, "Legendre fit to the reflection coefficient of a radiating rectangular waveguide aperture," *Antennas and Propagation, IEEE Transactions on*, vol. 60, pp. 4009 – 4014, aug. 2012.

[8] A. Ferrero and U. Pisani, "Two-port network analyzer calibration using an unknown 'thru'," *IEEE Microwave and Guided Wave Letters*, vol. 2, no. 12, pp. 505–507, 1992.

[9] Wikipedia, "Mobius transformation — wikipedia, the free encyclopedia," 2014. [Online; accessed 23-June-2014].

[10] J. Bauer, R.F. and P. Penfield, "De-embedding and unterminating," *Microwave Theory and Techniques, IEEE Transactions on*, vol. 22, pp. 282 – 288, mar. 1974.

[11] R. E. Collin, *Foundations for Microwave Engineering - 2nd edition*. Wiley-IEEE Press, 2000.

[12] B. Bianco, A. Corana, S. Ridella, and C. Simicich, "Evaluation of errors in calibration procedures for measurements of reflection coefficient," *Instrumentation and Measurement, IEEE Transactions on*, vol. 27, pp. 354 –358, Dec. 1978.

[13] C. Zwikker, *The Advanced Geometry of Plane Curves and Their Applications*. Mineola, N.Y: Dover Publications, Jan. 2005.

[14] C. Doran and A. Lasenby, *Geometric Algebra for Physicists*. Cambridge University Press, 2007.

[15] scikit-rf Development Team, "scikit-rf: Open source rf engineering," 2009-present. http://www.scikit-rf.org.

[16] R. B. Marks, "Formulations of the basic vector network analyzer error model including switch-terms," in *ARFTG Conference Digest-Fall, 50th*, vol. 32, pp. 115 –126, Dec. 1997.

[17] H.-J. Eul and B. Schiek, "A generalized theory and new calibration procedures for network analyzer self-calibration," *Microwave Theory and Techniques, IEEE Transactions on*, vol. 39, pp. 724 –731, apr. 1991.

[18] K. Wong, "Uncertainty analysis of the weighted least squares vna calibration," in *ARFTG Microwave Measurements Conference, Fall 2004. 64th*, pp. 23 – 31, 2-3 2004.

[19] R. F. Harrington, *Time-Harmonic Electromagnetic Fields (IEEE Press Series on Electromagnetic Wave Theory)*. Wiley-IEEE Press, 2001.